Drawbacks on the application of nozzle vanes in turbocharger turbine under pulsating flow conditions

M.H. Padzillah*[,1], S. Rajoo[1], R.F. Martinez-Botas[2]

[1]UTM Centre for Low Carbon Transport in Cooperation with Imperial College London
Universiti Teknologi Malaysia
81310 Johor, Malaysia

[2]Imperial College London
Exhibition Road, SW7 2AZ
London, United Kingdom

Abstract It is commonly agreed that a turbocharger turbine behaves differently between steady and pulsating flow operations. This is due in no small part to the flow field distribution within the turbine stage. The use of nozzle vanes has significantly increased the three-dimensional complexity of the flow field, although some argue that the use of such stator could lead to improved overall turbine performance. This research investigates the drawbacks on the circumferential flow angle distributions due to existence of nozzle vanes particularly during pulsating flow conditions. In achieving this objective, a validated full stage unsteady CFD model was built to gain insight of the flow field behaviour. The results indicate that application of nozzle vanes has favourable effect on flow angle distribution at the rotor inlet during steady state operations for both design and off-design conditions. This is achieved in such a way that the existence of nozzle vanes has reduced the fluctuation of flow angle as compared to the flow upstream the vanes. On the other hand, during pulsating flow turbine operation, the fluctuation amplitude has spiked almost 400% the level of its counterpart under steady state operation at the rotor inlet. This behaviour could

* Corresponding Author, Email: mhasbullah@utm.my

potentially have adverse effect on flow field distribution within the turbine passage and as such, reducing unsteady turbine efficiency.

Keywords: Pulsating flow, nozzle vanes, turbocharger turbine

1 Introduction

The application of nozzle vanes in a turbocharger turbine is currently a common practice in the automotive industry. In coping with ever stringent emission standard, many investigations have been conducted to maximize turbine efficiency by means of nozzle vanes. It has been claimed that the use right shaped vanes could improve flow structure at the rotor inlet thus increase the turbine performance [1]. Yadagiri et al. [1] investigated the influence of symmetrical and asymmetrical arrangement of vanes towards the turbine performance. They concluded that vanes with symmetrical arrangement cause higher pressure drop at lower speed thus compromise the turbine efficiency. Yadagiri et al. [1] later claimed that the use of asymmetric vanes could provide better exit flow angle for improved performance. Sakai et al. [2] attempted to improve the power extraction capability of the turbine by optimization of vanes arrangement that accommodates the need for EGR control under pulsating flow conditions. This is achieved by utilizing variable geometry vanes to optimize the flow at EGR side and no vanes at all at the other turbine entry. The results show promising efficiency improvement, although complex control methods for the vanes are needed for efficient operation. Furthermore, Liu et al. [3] proposed a low flow loss vanes that use leminscate shape and indicated significant overall turbocharger efficiency improvement. This promising work however is not experimentally validated. Albeit significant increment of complexity, Pesiridis [4, 5] and Rajoo and Martinez-Botas [6] has worked on the active controlled turbocharger (ACT) to actively adapt to the pulsating exhaust flow. The concept recorded a maximum value of 7.5% increase over the equivalent geometry turbocharger performance. However, this improvement is limited only to the most favourable amplitudes tested. The complexity of ACT concept in terms of its control strategies is well documented in [7, 8].

Meanwhile, study by Simpson et al. [9] has indicated that the use of vanes in general has resulted in higher losses as compared to vaneless turbines. This is due to high level of circumferential nonuniformity at the rotor inlet caused by the existence of vanes. It is also worthwhile to note that the study of Simpson et al. [9] is focused on steady state turbine operations. Romagnoli and Martinez-Botas [10] came up with a novel method of predicting the performance of both vaned and vaneless turbine. The model is able to predict the turbine performance with excellent accuracy and could also accommodate for change in vane angle setting. However, the work of Romagnoli and Martinez-Botas [10] is still limited to steady state turbine operations. For unsteady turbine operations, Padzillah et al. [11] indicated that there exist significant differences on the distribution of flow angle prior to entering the rotor wheel between vaned and vaneless turbocharger turbine. Padzillah et al. [11] found that the flow angle distribution in vaned volutes is more sensitive towards the incoming pulsating flow as compared to vaneless volutes. The outcome from this research demands further investigation to point out whether the use of vanes is beneficial during actual pulsating flow operations. Liu et al. [12] conducted a research to investigate the influence of nozzle openings of radial turbine under unsteady flow conditions. They indicated that small nozzle opening enhances the interaction between the tip leakage and wake flow. This in turn increases the risk of high cycle fatigue failure caused by aerodynamic excitation on the leading edge of the rotor. Furthermore, Natkaniec et al. [13] has performed and investigation on secondary flow structures and losses in a radial turbine nozzle. The rather computationally expensive simulation using 12.5 million nodes has indicated evidence of secondary vortices formation, as an addition to inflow and horse shoe vortices [14, 15].

From the available literature, it is safe to mention that the use of nozzle vanes has increase the level of flow field complexity in already complex turbocharger geometry. This research aims to visualize drawbacks of the nozzle vanes existence in terms of flow angle distribution across the volute circumference at the rotor leading edge.

2 Methodology

2.1 Experimental methodology

Figure 1 shows the schematics of the turbocharger test facility used in this research. The facility is located at Imperial College London and is used for cold-flow testing under steady and pulsating inlet conditions. The compressed air for the test rig is supplied by three screw-type compressors with capacity up to 1 kg/s at maximum absolute pressure of 5 bars. The air is heated by a heater-stack to the temperature between 330K to 345K to prevent condensation during gas expansion in the turbine. The flow is then channeled into two 81.40mm diameter limbs, namely outer and inner limb due to its relative position. This enables testing not only for single entry turbine but also for double or twin entry turbine. The mass flow rate in both limbs is measured using orifice plates. Downstream the orifice plates is a pulse generator originally designed by Dale and Watson [16] in 1986. The pulse generator enables actual pressure pulse in the exhaust manifold to be replicated in the facility with the frequency up to 80Hz. Downstream the pulse generator is the 'measurement plane', where all the parameters for the turbine inlet were acquired. This includes instantaneous total and static pressure sensors and thermocouples. A hotwire anemometer is also installed at the measurement planet to measure instantaneous mass flow rate.

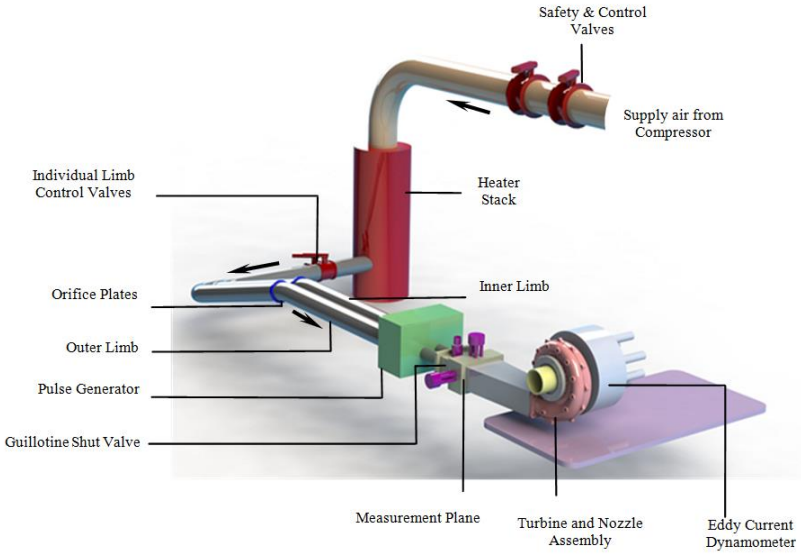

Figure 1: Schematics of the cold flow turbocharger test facility

The turbine is attached to a 60kW eddy current dynamometer where it is placed on a gimbal bearing. The details of the eddy current dynamometer design is provided by Szymko[17]. The reaction force on the dynamometer assembly is measured by a 20kg load cell where the torque is then calculated. The dynamometer also places a high flow rate water cooling system to disperse excessive heat absorbed by the magnetic plate. An optical sensor for instantaneous speed measurement is also installed within the dynamometer assembly.

2.2 Numerical methodology

The simulation works conducted in this research were executed using commercial software Ansys CFX 14.1. The 3-Dimensional turbocharger turbine geometry consists of 5 main components which are the inlet duct, a modified Holset H3B turbine volute [18], 15 NACA 0015 profiled vanes and a mixed flow turbine with 40mm chord length. The inlet duct and the volute were constructed using Solidworks and meshed using Ansys ICEM CFD. For the nozzle stage, 15 lean vanes were constructed by importing 3 profile lines into TurboGrid software where structured hexahedral meshed is automatically generated. Similar method is used to mesh the mixed flow turbine except 8 profile lines are needed due to its more complex geometry. The turbine used is an in-house turbine designated Rotor A created by Abidat [19] in 1991 for application in high loading operations. Figure 2(a) shows the resultant polynomial lines that forms hub (blue line) and shroud (red line) of the rotor wheel. Figure 2(b) shows the curvature for leading edge and camber line of the blade.

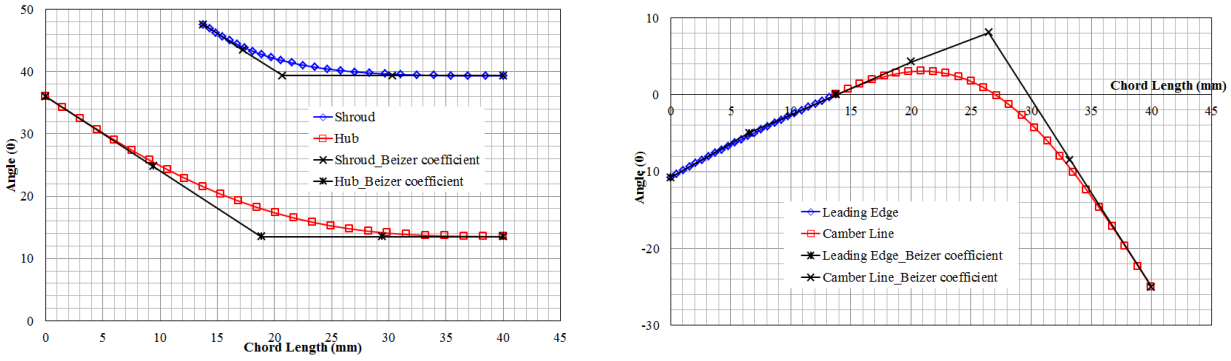

(a) (b)

Figure 2: (a) Hub and shroud and (b) Camberline profile generated from Bezier Polynomial

Subsequently, all meshed components were assembled in Ansys CFX-Pre as shown in Figure 3. The interfaces between each component are specified during this stage. The interfaces between inlet duct and volute, and also between volute to vane are specified as general connection. For steady state simulations, the 'frozen-rotor' interface is chosen as the interface between stationary and rotating domain. This assumes no relative motion during simulation and the information regarding rotor speed is embedded into a source term. Meanwhile, for unsteady flow simulation, the transient rotor-stator interface is specified between stationary and rotating domain to enable physical movement of the rotor for each timestep. The specified timestep is 1^{0} of rotor rotation per timestep and transient data are extracted for every 90^{0} turbine rotation. Simulations are allowed to run up to 3 pulse cycles to ensure cyclic convergence.

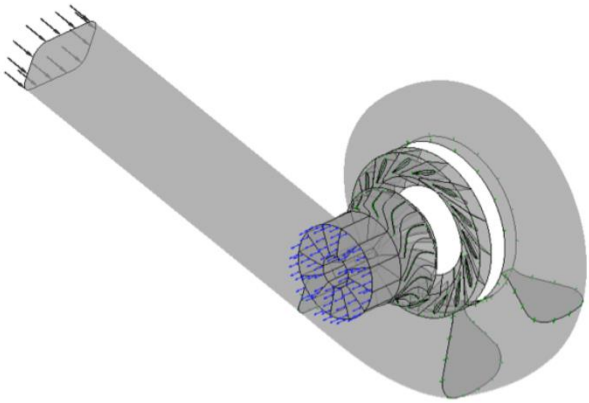

Figure 3: Assembly of the domains in CFX-Pre

For pulsating flow simulation, time varying total pressure and total temperature are specified at the domain inlet. The turbine speed of 30000 rpm which is equivalent to 50% design condition is selected. A flow frequency of 20 Hz is also specified during the initial setup. The original values for the boundary conditions were extracted from the experimental results. The direction of inlet flow is defined so that the only velocity component that exists is normal to the inlet plane. The outlet boundary condition requires the static pressure value. For this purpose, a constant atmospheric pressure is applied at the domain outlet. No-slip boundary condition is specified at all walls

including vanes and rotor blades. Similar boundary condition is used for steady state simulations with the exception of time varying pressure and temperature.

3 Results and discussion

3.1 Validation Exercises

The validation of simulation results were done in two phases. The first phase focuses on the validation of steady state simulation data. This process is followed by the second phase which focuses on unsteady simulation. Figure 4(a) shows the plot of mass flow parameter against pressure ratio for the turbine rotating at 30000 rpm. Both CFD and experimental data are plotted on similar axis to enable direct comparison. From the figure, it can be seen that the model used in this research are able to capture the trend and magnitude of the turbine mass flow parameter (also known as swallowing capacity) well for the entire operating range. The RMS of the deviation from experimental data is approximately 2%.

The validation procedure involving turbine efficiency has proven to be more difficult since efficiency is a derived parameter. Therefore, it depends on accuracy of several calculated parameter such as mass flow rate, torque, temperature and pressure. In addition, the use of fixed values such as the turbine speed and specific heat ratio could also lead to over or under prediction of turbine efficiency. Figure 4(b) shows the comparison between experimental data and CFD prediction of the turbine efficiency against velocity ratio. It can be seen that CFD tend to under-predict the efficiency value for velocity ratio less than 0.85. The maximum deviation is recorded to be 5 efficiency points at velocity ratio of 0.36. The RMS deviation recorded for this plot is 2 efficiency points. Minimal RMS for both plots indicated that the developed steady state model has achieved sufficient accuracy and as suc,h it is possible to proceed with the second phase validation process.

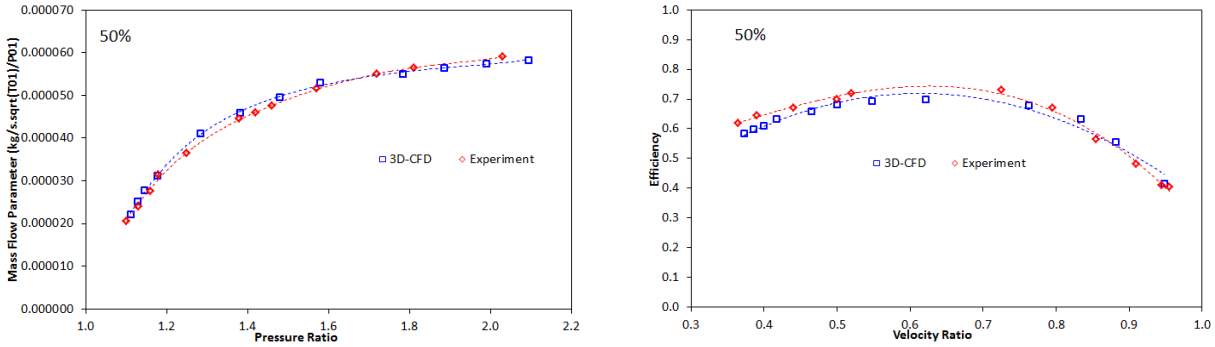

(a) (b)

Figure 4: Comparison between experimental and numerical data for (a) Mass Flow Parameter vs Pressure Ratio and (b) Efficiency vs Velocity Ratio

For the second phase of the validation exercises, unlike the validation procedures for steady state turbine operating condition where the chosen validation parameters are the derived quantities, the validation for pulsating turbine condition is focused on fundamental parameters. In this case, two parameters namely static pressure at 180^0 volute circumference and the turbine rotor torque have been selected. The selection of fundamental parameters instead of the turbine performance parameters is done in order to validate the parameters obtained by CFD to the parameters that are measured during the experimental works. This ensures that any deviations between CFD and experiment can be seen in time domain and a potential source of error could be determined.

Figure 5 shows the plot of static pressure at the centroid 180^0 volute circumference for both experiment as well as CFD calculation. It can be seen that CFD calculation is able to pick up the pressure trace well during the pressure increment and decrement instance, as well as the trough region of the pulse. In addition the calculated static pressure range also matched with the experimental data. However, at the pulse peak, CFD calculation shows some deviation in terms of the phase of the peak pressure. The peak pressure as indicated by CFD occurs about 10^0 phase angle later than that of experimental plot. Nevertheless, the magnitudes of both peaks are in good agreement to each other.

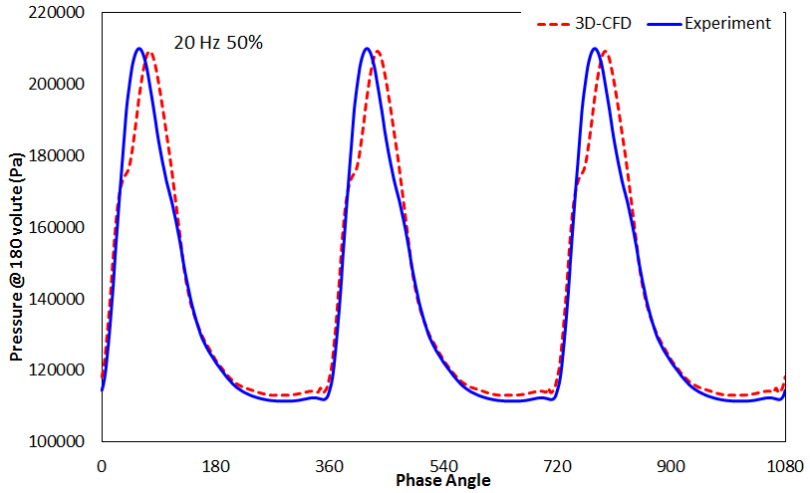

Figure 5: Comparison of static pressure at 180 volute circumference between experiment and CFD calculation

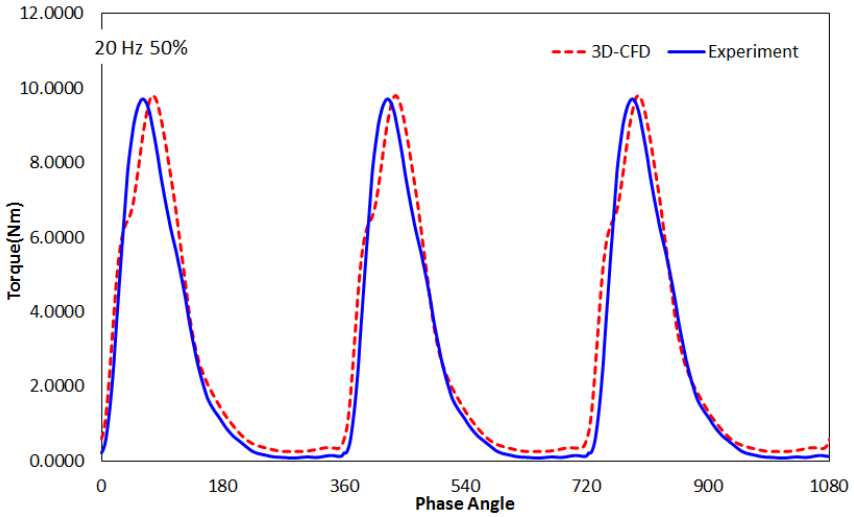

Figure 6: Comparison of rotor torque between experiment and CFD Calculation

Following the validation of pressure trace in the volute stage, another parameter which is directly related to the turbine wheel, namely torque is plotted in Figure 6. Overall, the CFD calculation agrees well with experimental data. The shifting of peak position that is seen previously in Figure 5 can still be seen in the torque trace while the magnitude of peak torque is still in agreement to each other. The validation of both parameters, despite slight shifting in the peak region still indicate that the developed

model is able to capture the time dependent pulsating flow within the turbocharger turbine stage. Therefore, the viability of the model for pulsating flow environment is confirmed and is used for further analysis.

3.2 Flow analysis

The analysis in this section focuses on flow angle distribution before and after the flow passes through the nozzle vanes. This ensures that any effect that the vanes has on the flow are well captured and appropriate assessment can be done to decide whether the vanes have adverse or favourable influence to the flow entering the turbine rotor. In achieving this, a reference case of turbine under its optimum condition during steady state operation is presented. Figure 8 shows the absolute flow angle distribution along the circumference of the volute at vane inlet and rotor inlet. The location where the flow angle at the volute exit is measured is detailed in Figure 7.

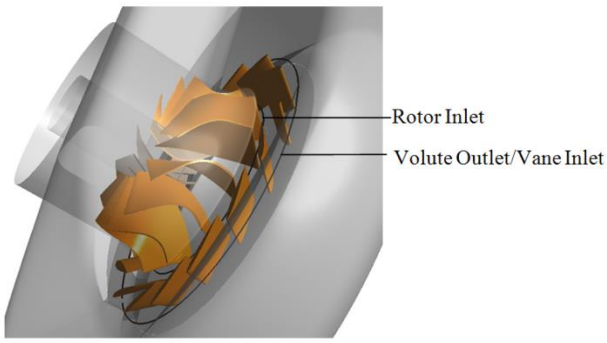

Figure 7: Locations for data measurements

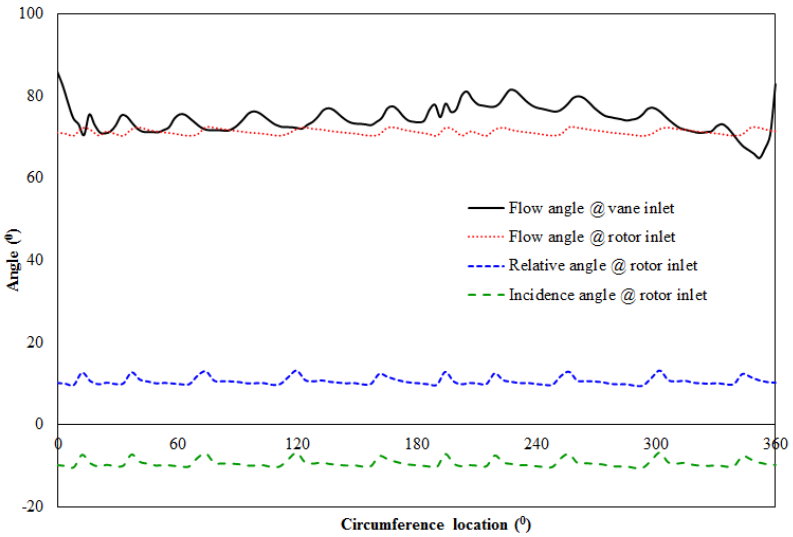

Figure 8: Flow angle distribution at vane inlet and rotor inlet along the volute circumference at 50% spanwise location during steady state operation

Downstream the volute exit, the flow is expected to enter the vane domain at a flow angle of 69^{0}. This value is selected during the design stage of the volute and is assumed to be constant throughout the exit of the volute circumference. However, this condition (constant flow angle) is seldom met due to the free vortex assumption that is utilized during the volute design stage. From Figure 8, it can be clearly seen that the flow angle entering the vanes does not maintain a constant value but it fluctuates due to the proximity of the vanes. Maximum fluctuation is recorded close to the tongue region with the magnitude of $\pm 10^{0}$.

As the flow passes through the vane, the flow angle variation across the circumferential location has reduced significantly as compared to its variation at the volute exit/vane inlet. At the exit of the vanes, only small localized fluctuations are detected due to proximity to the turbine wheel inlet. There are no evidence of the wake flow from the vanes trailing edge being seen at the location where the flow angle is measured. The magnitude of the mean flow angle is now 71^{0} with only $\pm 1^{0}$ fluctuation. This observation shows that current arrangement of vanes is sufficient to guide the flow and to minimize the substantial flow angle fluctuations that occur at the volute exit. This in turn ensures that the flow enters the rotor at a constant incidence angle which is very beneficial provided that the incidence angle falls into its optimum range. The relative and incidence angle are also plotted in the same axis in Figure 8 as reference.

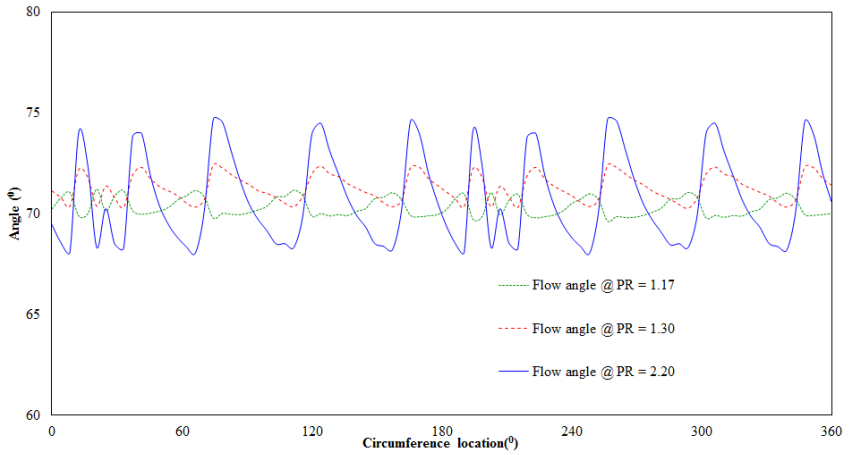

Figure 9: Plot of the absolute flow angle for 360 circumferential location at the rotor inlet for different steady state operating conditions

Several other cases under steady flow conditions are also presented to see the capability of the vanes to turn the flow at off-design operations. Figure 9 shows the absolute angle variation at mid span of the entire rotor inlet circumference for different operating conditions. It can be seen that for different operating conditions, the vanes are still able turned the flow to an average value of 71^0. However, it can also be seen that the increment in pressure ratio results in higher fluctuation range of the flow angle. For the particular turbine speed of 30000 rpm, the pressure ratio of 2.2 indicated 6^0 fluctuation range where the pressure ratio of 1.17 only indicated 1^0 fluctuation.

In order to analyse the unsteady flow field during pulsating operations of the turbine, a single pressure ratio during pressure increment and decrement instances of a pulse is selected. In addition to these two points, a similar pressure ratio under steady state operation is also chosen. The instance of selected conditions are detailed and visualized in Figure 10. *pt1* and *pt2* are taken at similar pressure ratio but at different instances whereas *pt3* is taken as the equivalent condition under steady state flow. The magnitude for *pt1* and *pt2* are selected at mid-range pressure between the lowest and the highest pressure in the particular operating condition.

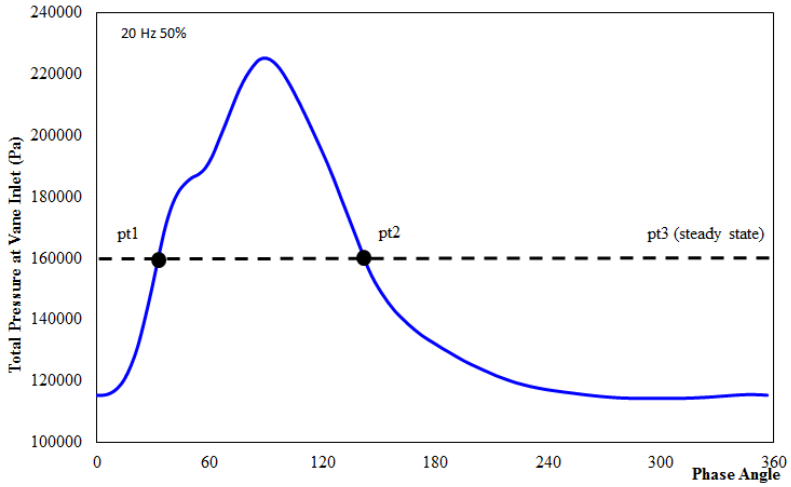

Figure 10: Unsteady and steady conditions for flow field analysis

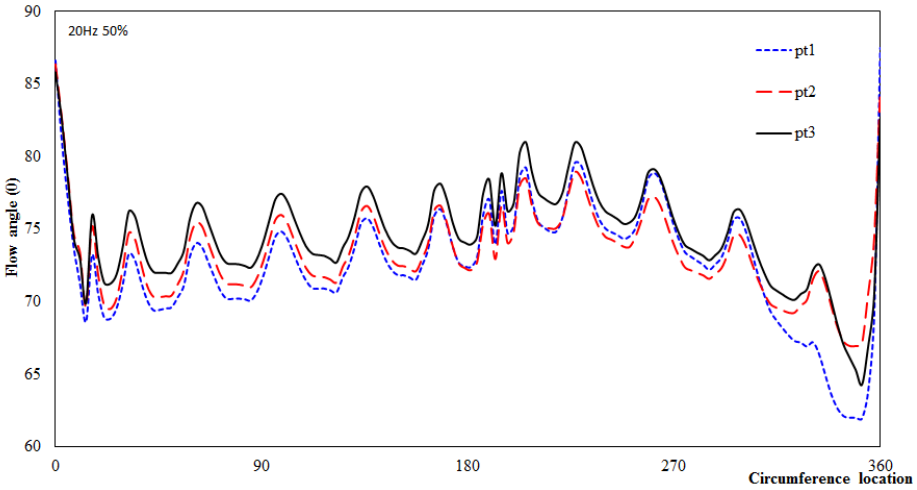

Figure 11: Flow angle distribution against the circumferential location of the vane inlet

Figure 11 shows the flow angle at the circumference of the vanes inlet for all three conditions. It is interesting to note that all three conditions indicated almost similar flow angle variation circumferentially. In general it can be seen that all three conditions indicated that the volute is capable of maintaining the flow angle at the average value of 73^0 from 0^0 until 200^0 circumferential position after which the flow angle drops gradually for about 10^0 before reaching the end of volute circumference. The minimum value of flow angle is recorded for *pt1* at 350^0 with the magnitude of 60^0. Meanwhile, large deviation towards high magnitude of flow angle occurs close to the tongue region (in the vicinity of 0^0 and 360^0). This behaviour is recorded for all three conditions.

This indicated that the flow close to the tongue is almost tangential regardless of the inlet conditions whether it is steady or pulsating flow.

It has been indicated earlier in Figure 8 during steady state operation analysis that the vanes are responsible to provide uniformly distributed absolute flow angle throughout the inlet circumference of the rotor. However, at the proximity of the rotor blade, the flow angle experienced changes due to the effect of back pressure. In an optimum steady flow operation, these changes are recorded to be less than $\pm 1^{0}$ from the mean value. Figure 12 shows the plot of circumferential distribution of absolute flow angle at the rotor inlet for all three operating conditions. It can be seen in that the although the average value of the flow angle at these conditions are relatively similar (72^{0}), there is a clear difference between the magnitude of flow angle deviation between steady (*pt3*) and unsteady conditions (*pt1* and *pt2*) as the flow approaches the rotor inlet. *Pt3* shows flow angle fluctuations in the range of 5^{0} as compared to the other two unsteady conditions which have almost 20^{0} in range, an increment of 400%. This magnitude of fluctuation is even more than the fluctuation during high pressure steady state condition indicated earlier in Figure 9 which is 6^{0}. It can also be seen that the fluctuation range of the flow angle under pulsating flow condition is similar regardless of its instances. It is therefore clear from Figure 12 that the introduction of pulsating flow has resulted in unfavourable condition in terms of flow angle distribution at the rotor inlet even though with the existence of guide vanes.

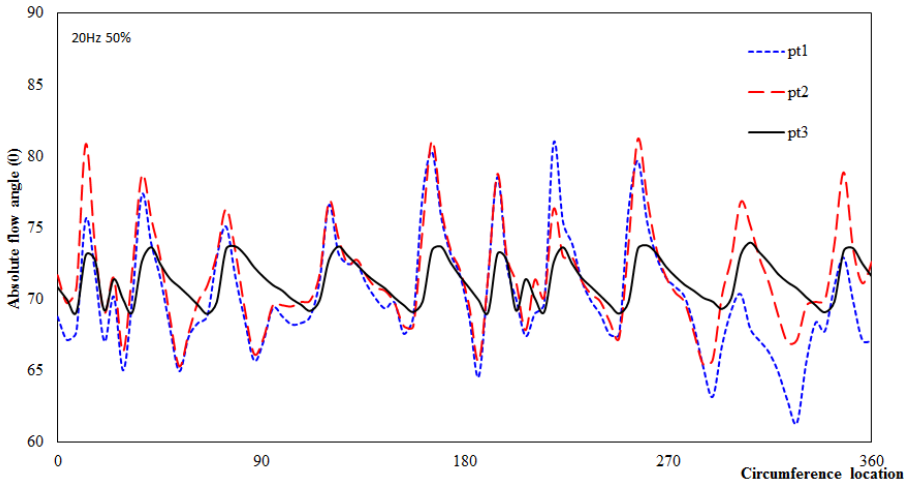

Figure 12: Absolute flow angle plot at the rotor inlet circumference

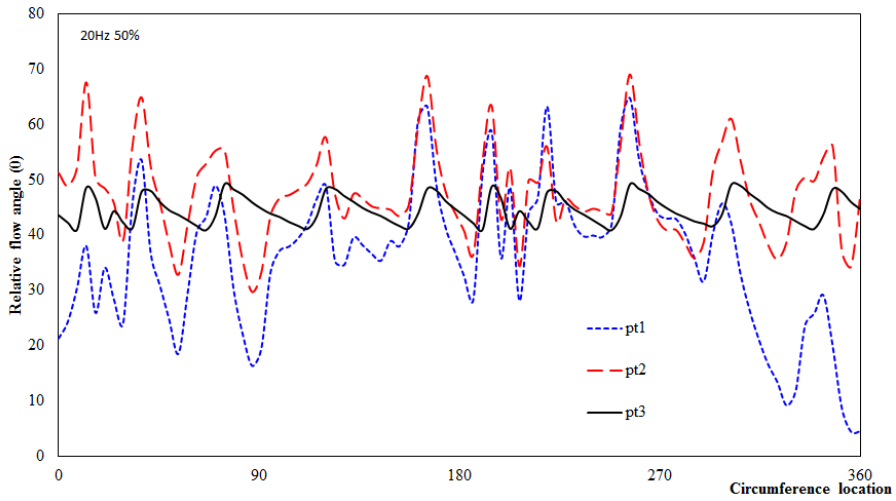

Figure 13: Relative flow angle plot at the rotor inlet circumference

The relative angle at the circumferential location of the rotor inlet for all three conditions is plotted in Figure 13. As all the conditions that are selected are at higher than optimum pressure ratio (1.3 during steady state condition), one would expect that the relative flow angle is positive in magnitude. In general, it can be seen in Figure 13 that the relative flow angle distribution for *pt1* and *pt2* are not as close together as their absolute flow angle distribution. It can be seen that *pt3* still maintain small range of fluctuations of the relative flow angle (8^0). *Pt1* indicated the most severe fluctuation compared to the other conditions. The range of relative flow angle fluctuation is up to 60^0 at this instance. Figure 13 also indicated that the initial expectation that pt1 and pt2 would operate closely due to similar pressure level at

inlet is incorrect. In fact, the relative flow angle at pt2 is larger at most of the circumferential location than pt1. Smaller fluctuation range is also recorded at pt2 as compared to pt1, indicating better circumferential distribution of the relative flow angle. The comparison with equivalent steady state condition (pt3) indicated that the relative flow angle during pressure decrement instance is likely to be closer to the steady state than during the pressure increment period. Additionally, during the pressure increment period (pt1), it can be seen that the tongue has a clear effect on relative flow angle where its value dropped very low (5^0) as the flow approaches 360^0 circumferential location. This feature ceases to exist at any other chosen conditions. This shows that the pulsating flow field has more influence in deteriorating the flow angle during pressure increment than during pressure decrement period.

4 Conclusion

A three dimensional full stage steady and unsteady CFD model has been constructed and validated. Results have revealed that the volute is sufficient to turn the flow to the desired angle for both steady and unsteady turbine operations. Furthermore, the fluctuations of flow angle recorded downstream the vane rows for unsteady flow (pressure increment and decrement instance) are 400% higher than that of steady flow. It is therefore concluded that the existence of guide vane helps stabilize the mean of flow angle during steady state operations; however it excites the flow angle fluctuations during unsteady turbine operations. This statement is true for both absolute and relative flow angle. It is also found that the flow angle distribution during pressure decrement instance is closer to that of steady state condition as compared to its distribution during pressure increment. In general, the application of nozzle vanes has its drawbacks in terms of flow angle distribution close to rotor inlet and therefore has adverse effect on the flow field within the rotor passage. This in turns could result in large formation of secondary flow and the inevitable efficiency penalty.

5 References

[1] Yadagiri Rapolu G, Balachandar SS, Kamaraj KV. 2014 Numerical Investigation: Effect of Stator Vanes on Turbocharger Turbine Performance. *Int. J. Rotating Mach.*, 2014, 1–11. Hindawi Publishing Corporation.

[2] Sakai M, Romagnoli A, Martinez-Botas RF. 2014 Performance and flow-field assessment of an EGR pulse optimised asymmetric double-entry turbocharger turbine. In *Institution of Mechanical Engineers - 11th International Conference on Turbochargers and Turbocharging*, Woodhead Publishing Limited. pp.321–332.

[3] Liu YG, Wang ZM, Hu YP, Li GX. 2006 Design of low flow loss nozzle vane of radial flow turbine. *J. Beijing Inst. Technol. (English Ed.*, 15(SUPPL.), 40–45.

[4] Pesiridis A. 2007 Turbocharger Turbine Unsteady Aerodynamics with Active Control. Imperial College of Science, Technology and Medicine, University of London.

[5] Pesiridis A. 2012 The application of active control for turbocharger turbines. *Int. J. Engine Res.*, 13(4), 385–398.

[6] Rajoo S, Martinez-Botas RF. 2007 Improving Energy Extraction from Pulsating Exhaust Flow by Active Operation of a Turbocharger Turbine. In *SAE Technical Papers*.

[7] Pesiridis A. 2012 Issues in the integration of active control turbochargers with internal combustion engines. *Int. J. Automot. Technol.*, 13(6), 873–884.

[8] Pesiridis A, Rajoo S. 2013 Variable Geometry Turbocharger Active Control Strategies for Enhanced Energy Recovery. In *SAE Technical Papers*.

[9] Simpson AT, Spence SWT, Watterson JK. 2009 A Comparison of the Flow Structures and Losses Within Vaned and Vaneless Stators for Radial Turbines. *J. Turbomach.*, 131(3), 031010.

[10] Romagnoli A, Martinez-Botas R. 2011 Performance Prediction of a Nozzled and Nozzleless Mixed-Flow Turbine in Steady Conditions. *Int. J. Mech. Sci.*, vol. 53, 557–574.

[11] Padzillah MH, Yang M, Zhuge W, Martinez-Botas RF. 2014 Numerical and Experimental Investigation of Pulsating Flow Effect on a Nozzled and Nozzleless Mixed Flow Turbine for an Automotive Turbocharger. In *Volume 2D: Turbomachinery*, ASME. p.V02DT42A027.

[12] Liu Y, Lao D, Liu Y, Yang C, Qi M. 2014 Investigation on the Effects of Nozzle Openings for a Radial Turbine with Variable Nozzle. In *SAE Technical Papers*, SAE International.

[13] Natkaniec CK, Kammeyer J, Seume JR. 2011 Secondary Flow Structures and Losses in a Radial Turbine Nozzle. In *Volume 3: Controls, Diagnostics and Instrumentation; Education; Electric Power; Microturbines and Small Turbomachinery; Solar Brayton and Rankine Cycle*, ASME. pp.977–987.

[14] Eroglu H, Tabakoff W. 1991 LDV measurements and investigation of flow field through radial turbine guide vanes. *J. Fluids Eng. Trans. ASME*, 113(4), 660–667. Publ by ASME.

[15] Hashemi SGR, Lemak RJ, Owczarek JA. 1984 INVESTIGATION OF THE FLOW CHARACTERISTICS AND OF LOSSES IN RADIAL NOZZLE CASCADES. *J. Eng. Gas Turbines Power*, 106(2), 502–510.

[16] Dale A, Watson N. 1986 Vaneless Radial Turbocharger Turbine Performance. *Proc. IMechE Int. Conf. Turbocharging Turbochargers (Mechanical Eng. Publ. London)*, 65–76.

[17] Szymko S. 2006 The development of an eddy current dynamometer for evaluation of steady and pulsating turbocharger turbine performance. Imperial College of Science, Technology and Medicine, University of London.

[18] Rajoo S. 2007 Steady and Pulsating Performance of a Variable Geometry Mixed Flow Turbochager Turbine. Imperial College of Science, Technology and Medicine, University of London.

[19] Abidat M. 1991 Design and Testing of a Highly Loaded Mixed Flow Turbine. Imperial College of Science, Technology and Medicine, University of London.